

# Mid-term Results of Freestyle Aortic Stentless Bioprosthetic Valve: Clinical Impact of Quantitative Analysis of In-vivo Three-dimensional Flow Velocity Profile by Magnetic Resonance Imaging

Hajime Matsue<sup>1</sup>, Yoshiki Sawa<sup>1</sup>, Goro Matsumiya<sup>1</sup>, Hikaru Matsuda<sup>1,3</sup>, Seiki Hamada<sup>2</sup>

<sup>1</sup>Division of Cardiovascular Surgery, Department of Surgery, <sup>2</sup>Department of Diagnostic Medicine, Osaka University Graduate School of Medicine, Osaka, Suita, Japan

<sup>3</sup>Present address: Hyogo Medical College

**Background and aim of the study:** The study aim was to investigate the in-vivo flow profiles of a stentless aortic bioprosthetic valve by MRI flow quantification, and to identify the clinical implication of prosthesis size and implantation method.

**Methods:** Twenty-six patients with a Freestyle stentless aortic bioprosthetic valve were studied using three-dimensional flow velocity profile by MRI, and compared with four patients with a stented aortic bioprosthetic valve and four healthy volunteers. Flow velocity profiles were analyzed quantitatively by the hydromechanics parameter, mean to peak velocity ratio at peak systole and compared with parameters monitored echocardiographically.

**Results:** In larger-sized valves or full root implantation, flow profiles showed an optimal pattern with low gradients, a high mean to peak velocity ratio, and

Among the current practices of valvular surgery, stentless aortic bioprostheses have been reported to provide superior hemodynamic performance. Low transvalvular gradients and a large effective orifice area (EOA), superior to that of stented bioprostheses and approximately similar to that for homograft valves and normal native valves, were advantageous, especially in patients with a small aortic root as this led to minimal prosthesis-patient mismatch (1-10). However, a subset of patients exhibited suboptimal hemodynamics with relatively high transvalvular gradients and small EOA (11,12). Although these hemodynamic parameters were normally assessed echocardiographically in clinical patients, this was insufficient for a detailed analysis of the in-vivo flow profile from the viewpoint of hydromechanics (13). Previously, an

minimum disturbance which approximated that of a normal valve. By contrast, a subset of patients, notably with 21 mm valves and subcoronary implantation, showed suboptimal flow pattern with high gradient and low mean to peak velocity ratio which approximated that of stented valves. The mean to peak velocity ratio was more strongly related to peak velocity than to the indexed effective orifice area.

**Conclusion:** Although stentless aortic bioprostheses have excellent hemodynamic performance, some patients show suboptimal results. This seems to occur more often when the subcoronary technique is used, and especially with 21-mm valves. Care must be taken when using the subcoronary technique with a 21-mm valve in patients with a small body surface area.

The Journal of Heart Valve Disease 2005;14:630-636

analysis was reported of in-vivo flow velocity profiles of stentless aortic bioprostheses using magnetic resonance imaging (MRI) (14). In that report, the flow profiles showed an optimal pattern, with minimum turbulence in most cases, though some patients showed a suboptimal pattern with moderate to severe turbulence due to prosthesis-patient mismatch or incomplete cusp opening by septal hypertrophy resulting in subaortic stenotic eccentric flow. The study aim was to identify the clinical role of the in-vivo flow profile by quantitative analysis in the assessment of late hemodynamic findings, by considering the optimum size and method of stentless Freestyle aortic valve replacement.

## Clinical material and methods

### Patients

Among 50 patients who underwent aortic valve replacement with a Freestyle aortic stentless bioprosthesis at Osaka University Hospital, 26 (16 males, 10 females) were studied using three-dimensional flow

---

Address for correspondence:

Hikaru Matsuda MD, Division of Cardiovascular Surgery, Department of Surgery, (E-1) Osaka University Graduate School of Medicine, 2-2 Yamada-oka, Suita, Osaka, 565-0871, Japan  
e-mail: h.matsuda@hyo-med.ac.jp

velocity quantification with velocity-encoding phase-contrast cine-MRI. The results were compared with those from four cases with stented bioprosthesis, and with four healthy volunteers. The aortic lesions were stenosis in 12 patients, regurgitation in seven, mixed in three, and infective endocarditis in four (native valve in two, prosthetic valve in two). The implantation techniques utilized were subcoronary (SC) in 15 patients (modified SC in 14, complete SC in one patient), root inclusion (Incl) in seven, and full-root (FR) in four. Concomitant graft replacement of the ascending aorta was performed in two patients. The valve sizes implanted were 21 mm (n = 5), 23 mm (n = 6), 25 mm (n = 5), 27 mm (n = 9) and 29 mm (n = 1), with the valve size selected being as close as possible to the actual annulus diameter. The mean time period between surgery and conduction of the MRI investigations was  $16 \pm 13$  months (range: 3 to 48 months).

Four patients with a stented bioprosthesis (Mosaic) and four healthy volunteers (four males; age range: 25 to 26 years) were included as controls. All patients were in NYHA functional class I or II, and the cardiac rhythm was sinus rhythm in all cases at the time of the investigation.

#### Flow velocity quantification by MRI

The details of this technique have been published previously (14). Measurements were made on a Siemens Magnetom Vision 1.5 Tesla superconducting MRI scanner. The patients were examined in the supine position using a CP Body Array coil. An electrocardiogram (ECG)-gated, dark-blood-prepared Turbo FLASH (Fast Low Angle Shot) sequence with three orthogonal slice packages was used to determine the orientation of the aortic prosthesis. A double-angulated FLASH cine image was acquired perpendicular to the aortic valve and parallel to the proximal ascending aorta to visualize the velocity jets and to adjust the slice position of the subsequent flow quantification downstream of the aortic prosthesis.

In order to quantify the velocity of the flow, the single-slice phase-contrast FLASH cine sequence with ECG-triggering was applied. Cine-phase velocity mapping was performed orthogonal to the ascending aorta approximately 20 mm (one annulus diameter) distal to the aortic prosthesis.

ECG-triggered two-dimensional velocity-encoded cine-phase contrast sequence was applied with an echo time (TE) of 4 ms. The maximum velocity was set at  $\pm 500$  cm/s. Through-plane velocity images allowed a distinction to be made between antegrade and retrograde flow perpendicular to the imaging plane. The slice thickness was 6 mm, the field of view was  $300 \times 300$  mm<sup>2</sup>, and the image matrix  $256 \times 256$ , resulting in an in-plane spatial resolution of  $1.17 \times 1.17$  mm<sup>2</sup>. The

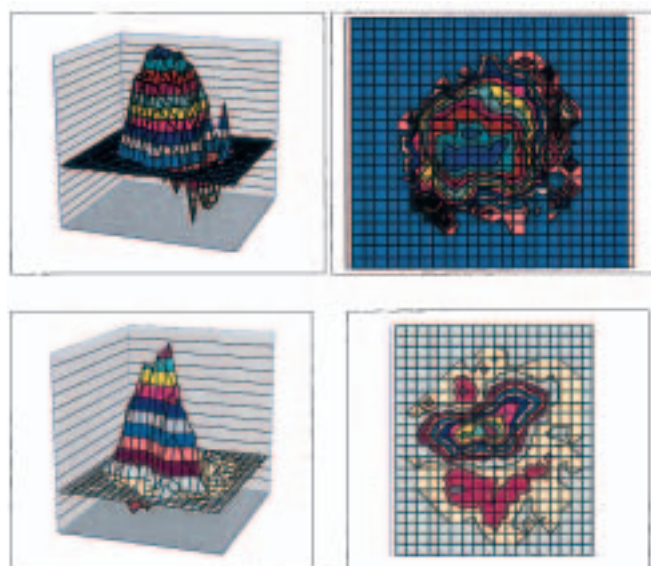


Figure 1: Three-dimensional flow profiles. Upper panels: Patient with Freestyle valve 29 mm using the full root technique. Lower panels: Patient with Freestyle valve 21 mm using the modified subcoronary technique. The flow profile was of optimal pattern with low velocity and high  $V_m/V_p$  ratio in the 29-mm valve, but was suboptimal in the 21-mm valve.

temporal resolution (i.e. the repetition time, TR) was 18 ms and the flip angle  $30^\circ$ . The number of excitation was 2; thus, the acquisition time was approximately 7-8 min for a heart rate of 70 beats per min.

#### Velocity data analysis

The data analysis was performed on a workstation (UltraSPARC-1 Creator; Sun Microsystems, Mountain View, CA, USA). To reduce artifacts, flow velocities were quantified automatically about every square voxel of  $2.4 \times 2.4$  mm<sup>2</sup>, which consisted of four pixels, in a rectangular region of interest (ROI), which circumscribes the aortic flow area, with a flow analysis software package developed at the authors' institution. Subsequently, the rectangular ROI was localized by vessel contours drawn manually on the corresponding normal cine image. The flow profiles were visualized by three-dimensional surface plots.

The peak velocity was calculated for each heart phase. Peak velocity was defined as the highest velocity value at the peak systolic phase.

The cross-sectional area at sampling plane (A), peak velocity ( $V_p$ ), and mean forward flow (rate per second, Q) were calculated at peak systolic phase. To allow a valid comparison of different subjects, the velocity axis was normalized by defining the peak velocity as 1.0. To

Table I: Characteristics of the study groups.

Parameter	Freestyle (n = 26)	Stented (Mosaic) (n = 4)	Healthy (n = 4)
Age (years)*	66 ± 9 (44-82)	73 ± 4 (68-77)	26 ± 1 (26-27)
Gender ratio (M/F)	16/10	2/2	4/0
BSA (m2)*	1.55 ± 0.17 (1.30-1.95)	1.55 ± 0.13 (1.40-1.74)	1.71 ± 0.05 (1.66-1.79)
Preoperative aortic lesion			
Stenosis	12	1	-
Regurgitation	7	1	-
Mixed	3	2	-
Infective endocarditis	4	0	-
Prosthetic valve size (mm)			
21	5	0	-
23	6	2	-
25	5	2	-
27	9	0	-
29	1	0	-
Implantation technique			
Subcoronary	15	-	-
Inclusion	7	-	-
Full root	4	-	-

\*Values are mean ± SD (range).  
BSA: Body surface area.

characterize the flow velocity profile, the hydraulic parameter of mean to peak velocity ratio ( $V_m/V_p$ ) was applied. The mean velocity ( $V_m$ ) was calculated as  $Q/A$ .

In hydromechanics, flow in a circular pipe is related to laminar flow and turbulent flow. In laminar flow, all fluid particles move parallel to the flow, and the flow profile is parabolic; hence  $V_m/V_p$  is 0.5. In turbulent flow, there are velocity components other than parallel, and these continuously change the velocity. Based on the power law equation (one of a number of semi-theoretical expressions for velocity distribution of turbulent flow in circular pipe), the velocity at any point in the cross-section is expressed as:

$$u_r/u_{CL} = (r/R)^{1/n} = (1 - r/R)^{1/n}$$

where  $u_r$  is the velocity at a distance  $r$  from the walls,  $u_{CL}$  is the velocity at the centerline of pipe, and  $R$  is the radius of the pipe. By using the Prandtl one-seventh power law, where  $n$  is seven,  $V_m/V_p$  was found to be equal to 0.817 times.

### Echocardiography

Echocardiography was performed within two weeks before or after MRI by the same physician, using an Agilent Technologies Sonos 2500 instrument, and according to the guidelines of the American Society of

Echocardiography. The details of echocardiographic measurements have been reported previously (13). The transvalvular peak velocity was measured using a continuous-wave Doppler technique in the apical view, and the EOA calculated using the continuity equation.

### Statistical analysis

All data were reported as mean ± SD. The unpaired Student's *t*-test was applied for comparisons of mean values between patients and normal volunteers. A *p*-value ≤0.05 was considered to be statistically significant.

## Results

### Flow profile

Flow profiles were successfully achieved in all cases. In the stented group, artifact due to the stent had no influence at the sampling plane.

As described previously, in the healthy group the flow profiles showed a superior flow pattern, with low velocity and minimum disturbance. In the Freestyle group, the flow profiles showed various disturbances from minimum as a healthy group to moderate or more (Fig. 1). Based on disturbances, the flow profiles were classified into three grades: grade A, minimum

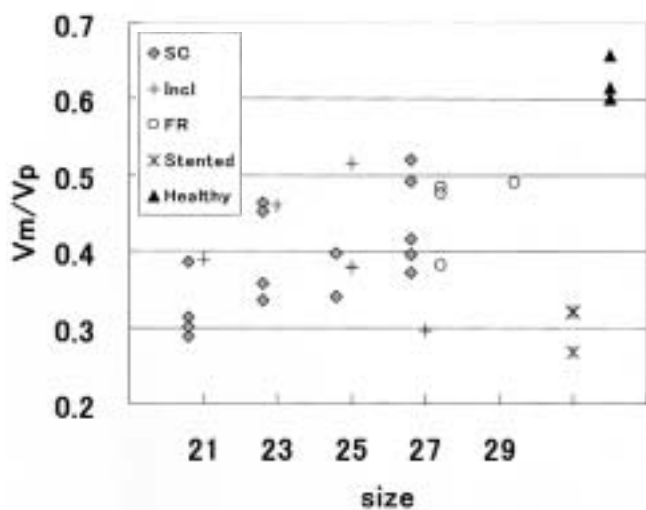


Figure 2: Relationship of mean to peak velocity ratio for valve type, size and implantation technique. Incl: Inclusion implantation; FR: Full root implantation; SC: Subcoronary implantation.

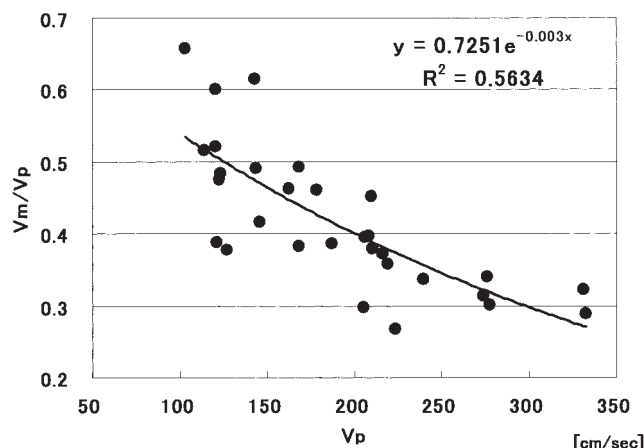


Figure 3: Relationship between peak velocity ( $V_p$ ) and mean to peak velocity ratio ( $V_m/V_p$ ).

disturbance; grade B, moderate disturbance; and grade C, severe disturbance. Among the Freestyle group ( $n = 26$ ), the flow profiles were classified as 13 grade A, nine grade B, and four grade C. In the stented group, all four cases showed severe disturbance and were classified as grade C.

#### Parameters of echocardiography and flow profile of MRI

Parameters of echocardiography and MRI in study group are shown in Table II. The indexed EOA was smaller in the stented group and 21-mm Freestyle subgroup. Although there was no significant difference in mean velocity between bioprosthesis sizes in the Freestyle group, the peak velocity was significantly higher the in smaller bioprosthesis size. The peak velocity was higher in the stented bioprosthesis and lower in healthy volunteers than in the Freestyle group.

#### Mean to peak velocity ratio

The mean to peak velocity ratio ( $V_m/V_p$ ) was smaller in 21 mm valves, especially when using the subcoronary technique (Fig. 2). In addition,  $V_m/V_p$  was larger than 0.5 in a subset of patients with 27 mm and 29 mm valves. The full root technique resulted in a larger  $V_m/V_p$  value. In the healthy group (which showed the ideal flow profile),  $V_m/V_p$  values were  $>0.6$ . In the stented bioprosthesis group,  $V_m/V_p$  was similar to that for the 21-mm valve, despite the bioprosthesis size being larger.

#### Peak velocity and mean to peak velocity ratio

The relationship between peak velocity ( $V_p$ ) and mean to peak velocity ratio ( $V_m/V_p$ ) is shown in Figure 3. Peak velocity increased exponentially with a decrease in mean  $V_m/V_p$ , regardless of valve type and size. It was suggested that the flow profile would be suboptimal when the peak velocity was higher ( $V_m/V_p = 0.7251e^{-0.003V_p}$ ;  $R^2 = 0.5634$ ).

#### Mean to peak velocity ratio and indexed EOA

Although  $V_m/V_p$  tended to increase with an increase in indexed EOA (Fig. 4), the relationship was not strong, suggesting that only the indexed EOA was insufficient to reveal the flow dynamics of the valves.

#### Clinical course of flow profile

In nine patients out of 26, repeated study of MRI flow profiles was performed within three months postoperatively and over a six-month period in general. During this time the grading of flow profiles was unchanged (Fig. 5).

The reduction in indexed left ventricular mass (LVM) and regression in relation to  $V_m/V_p$  after six months (or more) postoperatively is illustrated in Figures 6 and 7, respectively. The LVM index was significantly decreased. Although there was no significant relationship between the percentage LVM regression and the  $V_m/V_p$  ratio, regression tended to be greater when  $V_m/V_p$  was larger.

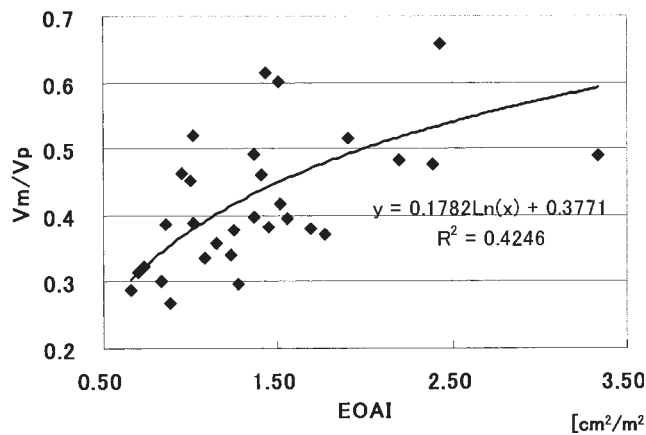


Figure 4: Relationship between indexed effective orifice area (EOAI) and mean to peak velocity ratio ( $V_m/V_p$ ).

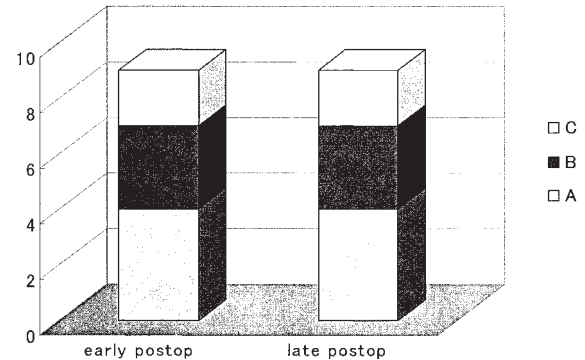


Figure 5: Grading of flow profiles at early (within 3 months) and late (>6 months) postoperatively in nine cases. Grade A = minimum disturbance; grade B = moderate disturbance; and grade C = severe disturbance.

## Discussion

Superior hemodynamics and satisfactory mid-term clinical results and durability of stentless aortic bioprosthetic valves have been reported. A lower transvalvular gradient and a larger EOA would be advantageous for LVM regression and survival, especially in those patients with a small aortic root or poor

left ventricular function.

By contrast, the optimal sizing and implantation technique for stentless aortic bioprosthetic valves is not understood sufficiently. It has been reported in one in-vitro study that oversizing and full root and inclusion implantation resulted in excellent hemodynamics (3), though the results of another in-vitro study suggested that a slight undersizing was better.

Table II: Parameters monitored by echocardiography and MRI.

Parameter	Freestyle valve					Stented	Healthy
	21 mm	23 mm	25 mm	27 mm	29 mm		
Patients (n)	5	6	5	9	1	4	4
EOA (cm <sup>2</sup> )	1.15 ± 0.13 (1.00-1.35)	1.60 ± 0.21 (1.38-1.95)	2.25 ± 0.17 (2.00-2.48)	2.68 ± 0.73 (1.82-4.51)	5.90 -	1.05 ± 0.22 (0.83-1.28)	3.49 ± 1.01 (2.39-4.64)
EOAI (cm <sup>2</sup> /m <sup>2</sup> )	0.81 ± 0.13 (0.66-1.01)	1.12 ± 0.16 (0.95-1.41)	1.49 ± 0.27 (1.23-1.90)	1.61 ± 0.41 (1.01-2.38)	3.33	0.66 ± 0.07 (0.59-0.73)	2.04 ± 0.59 (1.43-2.79)
$V_m$ (m/s)	0.77 ± 0.17 (0.47-0.96)	0.82 ± 0.07 (0.76-0.95)	0.73 ± 0.17 (0.48-0.94)	0.69 ± 0.10 (0.58-0.83)	0.72	0.83 ± 0.23 (0.60-1.07)	0.85 ± 0.17 (0.67-1.11)
$V_p$ (m/s)	2.38 ± 0.75 (1.21-3.33)	2.02 ± 0.28 (1.63-2.39)	1.87 ± 0.60 (1.14-2.76)	1.64 ± 0.36 (1.20-2.16)	1.44	2.78 ± 0.54 (2.24-3.31)	1.22 ± 0.15 (1.08-1.44)
Q (ml/s)	341 ± 73 (245-448)	398 ± 68 (333-499)	369 ± 103 (232-527)	423 ± 65 (282-516)	623	510 ± 158 (351-668)	458 ± 65 (371-543)
A (cm <sup>2</sup> )	4.5 ± 0.5 (3.8-5.2)	4.9 ± 1.0 (3.5-6.4)	5.1 ± 0.5 (4.2-5.6)	6.2 ± 1.0 (4.7-8.0)	8.7	6.1 ± 0.2 (5.9-6.3)	5.48 ± 0.55 (4.89-6.32)
$V_m/V_p$	0.34 ± 0.04 (0.29-0.39)	0.41 ± 0.06 (0.34-0.46)	0.40 ± 0.06 (0.34-0.52)	0.43 ± 0.06 (0.34-0.52)	0.49	0.29 ± 0.03 (0.27-0.32)	0.65 ± 0.04 (0.60-0.71)

Values are mean ± SD (range).

A: Cross-sectional area; EOA: Effective orifice area; EOAI: Indexed effective orifice area; Q: Mean forward flow;  $V_m/V_p$ : Mean to peak velocity ratio;  $V_m$ : Mean velocity;  $V_p$ : Peak velocity.

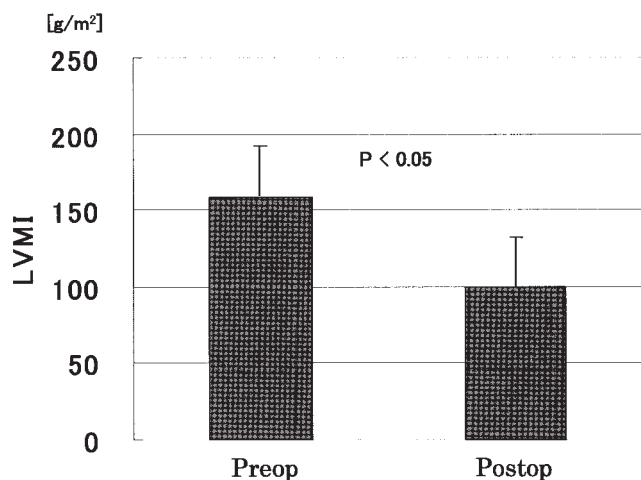


Figure 6: Regression of left ventricular mass index (LVMI), preoperatively and postoperatively. The LVMI was significantly reduced ( $p < 0.05$ ).

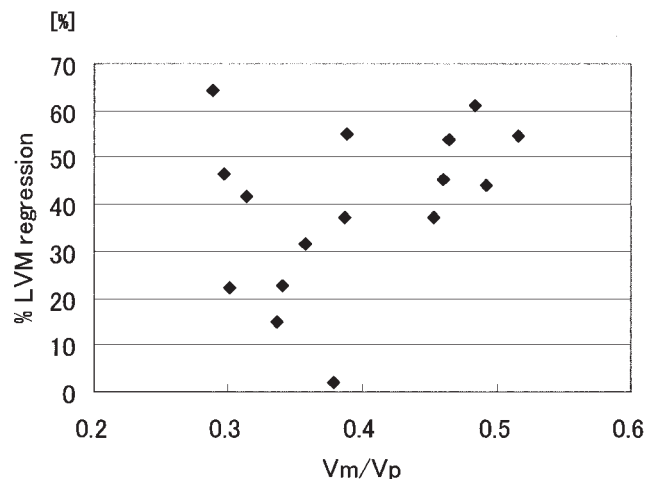


Figure 7: Relationship between mean to peak velocity ratio ( $V_m/V_p$ ) and percentage left ventricular mass (LVM) regression.

In clinical cases, however, hemodynamic performance will be affected by a variety of factors, and is more complicated than the in-vitro situation (16). The EOA and transvalvular gradient have a broader spectrum and are relatively inferior compared to in-vitro studies, and a small number of patients have been found to have suboptimal hemodynamics. The implications of these findings are not fully understood echocardiographically, however.

Three-dimensional flow quantification, when assessed by MRI, revealed more detailed characteristics of blood flow through the valves from the viewpoint of hydromechanics. A variety of grades of disturbance was highlighted in the present study. The  $V_m/V_p$  ratio was the most important indicator (hydromechanically) of flow profile, and was used to quantify the characteristics of the flow profiles. It was suggested that a flow profile might be preferable in cases with a lower gradient demonstrated by echocardiography. A larger-sized bioprosthesis showed a better profile, whilst a smaller bioprosthesis was relatively poor, especially in the case of 21-mm valves. In the present study, three patients with 21-mm valves, and all four with stented valves, showed small indexed EOA values ( $< 0.85 \text{ cm}^2/\text{m}^2$ ) and prosthesis-patient mismatch (17-19). With regard to the implantation technique utilized, although an analysis was possible only for a small number of cases, full root implantation appeared to be advantageous. The findings of the analysis of flow profiles appeared to be due to some degree of obstruction to flow and flow separation at the level of the aortic valve prosthesis, though this may reflect prosthesis-patient mismatch and incomplete opening of the cusp. In this respect, many

factors are involved, including valve size, implantation technique and aortic root geometry or distensibility.

Normal native aortic valves will have the ideal hemodynamic performance with the ideal flow profile. In the present study, the flow profiles in the healthy groups showed a lower gradient and larger EOA with a higher mean to peak velocity ratio.

In conclusion, the Freestyle stentless aortic bioprosthesis showed favorable hemodynamics and mid-term results in general. The flow profiles assessed by MRI were shown to be superior to those of stented bioprostheses, and to approximate those of a normal native valve, especially when using the full root technique and in some patients with a larger-sized bioprosthesis. However, a subset of patients showed a suboptimal flow profile and hemodynamics. Suboptimal hemodynamics appeared to occur more often in association with the subcoronary technique, especially with 21-mm valves. Thus, care will be needed when using the subcoronary technique with a 21-mm valve in patients with a smaller body surface area. This is the first report of a quantitative analysis of in-vivo flow profile of stentless aortic bioprosthesis, and the findings should be valuable when selecting an implantation technique and valve size. Moreover, they should also provide important information for bioprosthesis development.

#### References

1. Bach DS, Kon ND, Dumesnil JG, Sintek CF, Doty DB. Eight-year results after aortic valve replacement with the Freestyle stentless bioprosthesis. *J Thorac Cardiovasc Surg* 2004;127:1657-1663
2. Dumesnil JG, LeBlanc MH, Cartier PC, et al. Hemodynamic features of the Freestyle aortic bio-

- prosthesis compared with stented bioprosthesis. *Ann Thorac Surg* 1998;66:S130-S133
3. Yoganathan AP, Eberhardt CE, Walker PG. Hydrodynamic performance of the Medtronic Freestyle aortic root bioprosthesis. *J Heart Valve Dis* 1994;3:571-578
  4. Ohtake S, Sawa Y, Sakaguchi T, et al. Early experience of aortic valve replacement with Freestyle stentless aortic bioprosthesis in elderly patients. *Jpn J Thorac Cardiovasc Surg* 2000;48:222-228
  5. Sakaguchi T, Sawa Y, Ohtake S, Hirata N, Matsuda H. The Freestyle stentless bioprosthesis for prosthetic valve endocarditis. *Ann Thorac Surg* 1999;67:553-555
  6. Sawa Y, Matsuda H. Efficacy of aortic valve replacement with Freestyle stentless valve in patients with aortic valve disease. *Kyobu Geka* 2000;53:319-322
  7. Westaby S, Horton M, Jin XY, et al. Survival advantage of stentless aortic bioprostheses. *Ann Thorac Surg* 2000;70:785-790
  8. Akar AR, Szafranek A, Alexiou C, et al. Use of stentless xenografts in the aortic position: Determinants of early and late outcome. *Ann Thorac Surg* 2002;74:1450-1457
  9. Kappetein AP, Braun J, Baur LHB, et al. Outcome and follow-up of aortic valve replacement with Freestyle stentless bioprosthesis. *Ann Thorac Surg* 2001;71:601-608
  10. David TE, Feindel CM, Scully HE, Bos J, Rakowski H. Aortic valve replacement with stentless porcine aortic valves: A ten-year experience. *J Heart Valve Dis* 1998;7:250-254
  11. Bach DS, LeMire MS, Eberhart D, et al. Impact of high transvalvular velocities early after implantation of Freestyle stentless aortic bioprosthesis. *J Heart Valve Dis* 2000;9:536-543
  12. Bach DS, Cartier PA, Kon N, Johnson KG, Dumesnil JG, Doty DB. Impact of high transvalvular to subvalvular velocity ratio early after aortic valve replacement with Freestyle stentless aortic bioprosthesis. *Semin Thorac Cardiovasc Surg* 2001;13(Suppl.1):75-81
  13. Baur LH, Jin XY, Houdas Y, et al. Echocardiographic parameters of the freestyle stentless bioprosthesis in aortic position: The European experience. *J Am Soc Echocardiogr* 1999;12:729-735
  14. Matsue H, Sawa Y, Takahashi T, et al. Three-dimensional flow velocity quantification of Freestyle aortic stentless bioprosthesis by magnetic resonance imaging: Surgical consideration. *Semin Thorac Cardiovasc Surg* 2001;13(4 Suppl.1):60-66
  15. Nagy ZL, Fisher J, Walker PG, Watterson KG. The effect of sizing on the in vitro hydrodynamic characteristics and leaflet motion of the Toronto SPV stentless valve. *J Thorac Cardiovasc Surg* 1999;117:92-98
  16. Kon ND, Westaby S, Amarasena N, Pillai R, Cordell AR. Comparison of implantation techniques using Freestyle stentless porcine aortic valve. *Ann Thorac Surg* 1995;59:857-862
  17. Pibarot P, Dumesnil JG. Hemodynamic and clinical impact of prosthesis-patient mismatch in the aortic valve position and its prevention. *J Am Coll Cardiol* 2000;36:1131-1141
  18. Rao V, Jamieson WRE, Ivanov J, Armstrong S, David TE. Prosthesis-patient mismatch affects survival after aortic valve replacement. *Circulation* 2000;102 (Suppl.III):III5-III9
  19. Pibarot P, Dumesnil JG, Jobin J, Cartier P, Honos G, Durand LG. Hemodynamic and physical performance during maximal exercise in patients with an aortic bioprosthetic valve. Comparison of stentless versus stented bioprostheses. *J Am Coll Cardiol* 1999;34:1609-1617